

Hyperfine structure and radiative-lifetime determination for the $4d^{10}6p^2P$ states of neutral silver using pulsed laser spectroscopy

J. Bengtsson, J. Larsson, and S. Svanberg

Department of Physics, Lund Institute of Technology, P.O. Box 118, S-221 00 Lund, Sweden

(Received 9 February 1990)

The hyperfine structure and radiative lifetime of the $4d^{10}6p^2P$ states of neutral silver were determined in pulsed level-crossing, optical-double-resonance, and time-resolved experiments using high-power frequency-tripled radiation from a dye laser. For the $^2P_{3/2}$ state, we obtained $\tau=78(5)$ ns for the lifetime and $|a|=9.05(25)$ MHz for the magnetic-dipole interaction constant of ^{107}Ag . The lifetime and the a factor for the $^2P_{1/2}$ state were determined to be $\tau=95(6)$ ns and $|a|=38.7(10)$ MHz, respectively, using time-resolved laser spectroscopy. The experimental results are compared with theoretical calculations using the multiconfiguration Hartree-Fock method.

I. INTRODUCTION

The ground configuration of silver is $4d^{10}5s$. Excitation of the $5s$ electron results in a doublet energy-level scheme similar to that in rubidium. However, the closed $4d$ shell can easily be broken up, resulting in a large number of additional levels. A simplified energy-level diagram for silver with some transitions indicated is given in Fig. 1.^{1,2} Compared with the copper atom with a similar electronic structure, the $4d^95s5p$ configuration lies higher in energy relative to the doublet sequences and causes less dramatic perturbations for the lower doublets than for the strongly perturbed copper atom. The copper atom has recently been extensively investigated by our group, both experimentally³⁻⁵ and theoretically.⁶ A theoretical study of the Ag energy-level structure and radiative lifetimes is now under way at our laboratory.⁷ Very little accurate information on hyperfine structure (hfs) and radiative lifetimes of excited silver states exists. The $4d^{10}5p^2P_{3/2}$ state has been studied by level-crossing (LC) spectroscopy.^{8,9} The lifetime of the corresponding $^2P_{1/2}$ level was determined in an LC experiment by Soltanolkabi and Gupta.¹⁰

Improved data for the $5p^2P_{3/2,1/2}$ states were recently obtained in an investigation using time-resolved spectroscopy.¹¹ Lifetime measurements for a number of excited states have been performed by Plekhotkina¹² using electron excitation. An extensive study of radiative lifetimes in the 2S and 2D sequences has been performed by our group.¹³

In the present work we have been able to extend high-resolution measurements to the $4d^{10}6p^2P_{3/2,1/2}$ levels. In this way, we have substantially increased the number of excited silver states for which a comparison between experimental and theoretical hyperfine structure data can be performed. This is important since silver, like copper, provides the natural increment in the level of theoretical complication over the alkali-metal atoms which are now quite well understood. For silver, relativistic effects can be expected to play a more important part than for the lighter copper atom. The present work is part of an ongoing effort in our laboratory to develop powerful, general purpose high-resolution spectroscopic techniques applicable in the uv and vacuum ultraviolet (vuv) regions. This is achieved by employing pulsed lasers in combina-

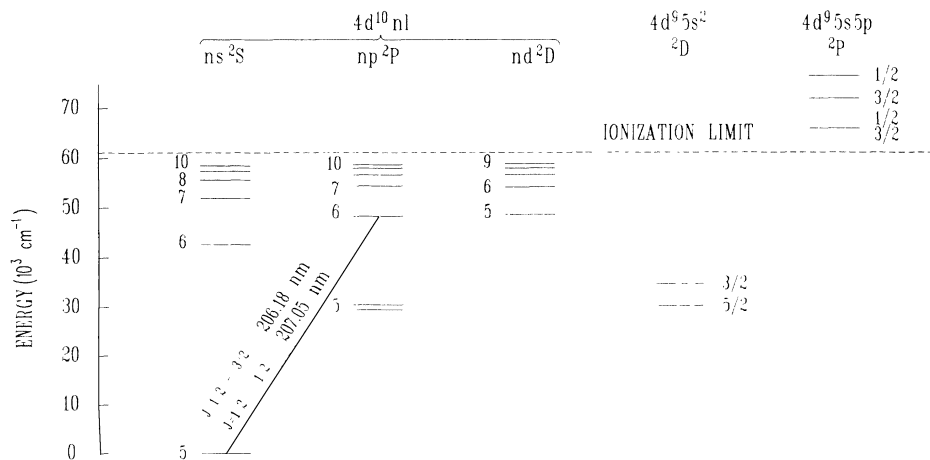


FIG. 1. Partial energy-level diagram for the silver atom with relevant transitions indicated.

tion with techniques for which the bandwidth of the laser presents no limitation. Such techniques are level-crossing and quantum-beat (QB) spectroscopy. In a previous paper,⁵ we discussed this concept in more detail. In the present work we have also applied optical-double-resonance (ODR) spectroscopy in a pulsed version. This has allowed us to increase the resolution, even beyond the Heisenberg limit, using delayed detection.

The $4d^{10}6p^2P_{3/2,1/2}$ levels in silver are connected to the ground state by lines at 206.2 and 207.1 nm, respectively. Laser light of this short wavelength was obtained by the frequency tripling of a pulsed high-power dye laser. LC and ODR measurements were performed for the $6p^2P_{3/2}$ state and QB experiments for the $6p^2P_{1/2}$ state. Time-resolved studies of the fluorescence decay also yielded the radiative lifetimes of the both members of the $6p$ doublet. Natural silver contains two isotopes, ^{107}Ag (51.8%) and ^{109}Ag (48.2%). Both isotopes have a nuclear spin of $I = \frac{1}{2}$, and thus the only hyperfine manifestation possible is the magnetic-dipole interaction. A diagram of the energy-sublevel structure for the $6p^2P_{3/2}$ state of ^{107}Ag as a function of an external magnetic field B is given in Fig. 2. An inverted hyperfine structure is indicated corresponding to negative magnetic moments for the silver isotopes. The $\Delta m = 2$ level crossings between sublevels with quantum numbers F, m , and F', m' are indicated. The diagram is the same for the ^{109}Ag isotope, except that the energy and magnetic-field scales are increased by a factor of 1.150, corresponding to the ratio between the two magnetic moments obtained from nuclear magnetic-resonance measurements.¹⁴ At the level

crossings the scattered fluorescence light will change its angular distribution, and this can be used to localize the crossing positions in level-crossing spectroscopy.¹⁵⁻¹⁸ The trivial level crossing at zero magnetic field (the Hanle effect) is particularly strong and can be used to determine the lifetime of the state.

In the Paschen-Back region of the hyperfine structure, rf transitions are indicated according to the selection rules $\Delta m_J = \pm 1$ and $\Delta m_I = 0$ (Fig. 2). The Paschen-Back level energies are given by

$$E_{m_J m_I} = m_J g_J \mu_B B - m_I g_I' \mu_B B + a m_I m_J,$$

where g_J is the Landé factor, g_I' is the nuclear g factor in Bohr magnetons, μ_B is the Bohr magneton, and a is the magnetic-dipole interaction constant.

Allowed rf transitions occur for

$$\Delta E = h\nu = g_J \mu_B B + a m_I.$$

Thus $2I + 1$ resonances are expected and are symmetrically placed around a center of gravity corresponding to the pure fine-structure position, which is determined by the g_J factor only. Thus for Ag with $I = \frac{1}{2}$ two signals are expected in the Paschen-Back region. The ODR method is used to optically detect the rf resonances.^{18,19} In Secs. II and III our experimental setup and measurements are described. The results are discussed in view of a multiconfiguration Hartree-Fock (MCHF) calculation in Sec. IV.

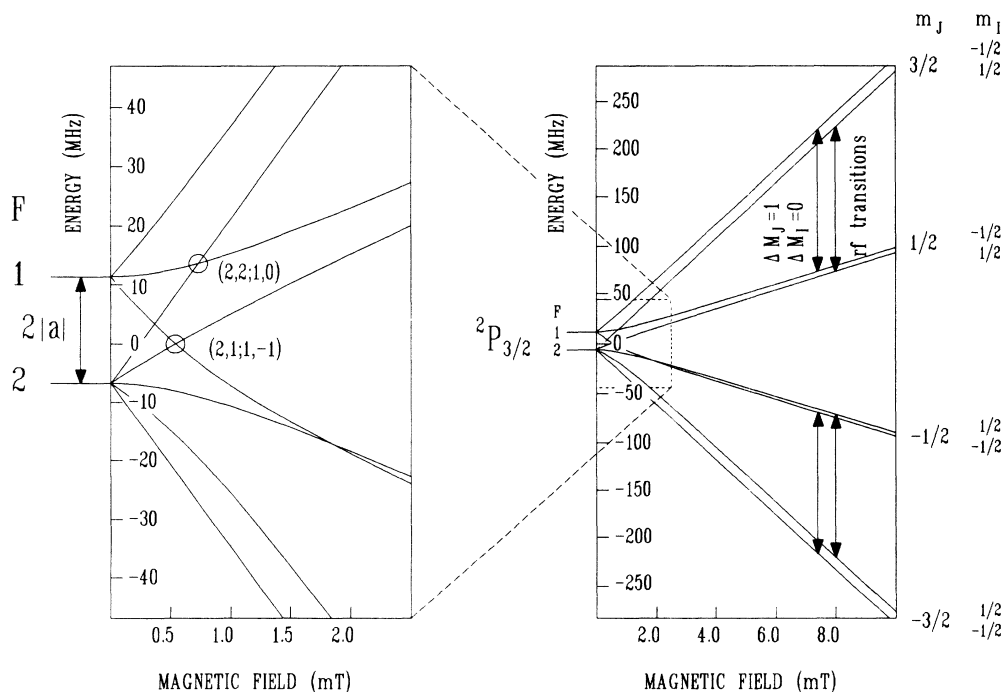


FIG. 2. Sublevel structure as a function of an external magnetic field for the $^2P_{3/2}$ state of ^{107}Ag . $\Delta m = 2$ level crossings are indicated using the symbols $(F, m; F', m')$ designating the low-field quantum numbers for the participating sublevels. rf transitions in the Paschen-Back region of the hfs are also indicated.

II. EXPERIMENTAL SETUP

The experimental setup shown in Fig. 3 is based on that described in connection with our recent experiments on copper.⁵ A Quantel Datachrome 5000 system was used for excitation. A Nd:YAG-pumped dye laser (where YAG is yttrium aluminum garnet) delivered high-power pulses of tunable radiation of about 10 ns duration at a repetition rate of 10 Hz. In order to obtain the short excitation wavelengths around 206 nm, dye-laser radiation at about 618 nm was first frequency doubled in a KDP (potassium dihydrogen phosphate) crystal and then mixed with the fundamental frequency in a BBO (β -barium borate) crystal to effectively produce the third harmonic of the dye-laser frequency. To accomplish the mixing a mechanically compressed crystalline quartz plate was used to rotate the fundamental and the doubled dye-laser radiation to obtain parallel polarization components before the BBO crystal. In our experiments pulse energies of about 3 mJ could be achieved. At the peak of the Rh 640 dye, energies approaching 10 mJ could be obtained.

The silver atoms were produced as a beam from an oven in a vacuum system. Two pairs of Helmholtz coils produced a magnetic field. The coil systems could be used to produce a static off-set field from which a periodic sweep field could be generated for repetitive data accumulation in our detection system. For the LC measurements, the geometry and polarizations of the excitation and detection beams were chosen for the detection of $\Delta m = 2$ crossing signals.

In ODR measurements we frequently used π ($\Delta m = 0$) excitation and employed σ ($\Delta m = \pm 1$) detection. rf transitions were induced by a two-turn coil connected to the

rf equipment. The output of a General Radio 1215-C unit oscillator was amplified in a Boonton Radio 230A tuned amplifier. Normally, we operated close to 144 MHz so that a 2-m amateur band power amplifier could be used to further boost the rf power. The frequency of the system was measured with a Hewlett-Packard 5300B frequency counter. In order to reduce the mean power dissipation in the final amplifier and in connecting cables, which tended to become overheated, the system was chopped in synchronization with the laser system with a duty cycle of about 10%. The fluorescence light was detected in the decay back to the ground state. At this short uv wavelength an efficient polarizer was achieved by using a stack of Suprasil quartz plates at Brewster's angle.

In the LC and ODR experiments EMI 9558 QA photomultipliers were used while a very fast Hamamatsu 1564U microchannel plate photomultiplier tube was employed for recording time-resolved fluorescence decay curves. A Stanford Research SR 265 boxcar integrator or a Tektronix DSA602 transient recorder connected to an IBM-compatible AT computer was used for data collection and processing. In some of the experiments the fluorescence was detected in two directions and the signals were divided to improve the signal-to-noise ratio, which is important when using pulsed lasers which have rather large pulse-to-pulse fluctuations.⁵ In order to compensate for detector nonlinearities and imperfect zero setting in the detector channels, we implemented a signal normalization routine first used by Wolf and Tiemann.²⁰ The detection system was first set in a "learning" mode in which the signals from both detectors were digitized and plotted versus each other, as illustrated in Fig. 4. A linear or polynomial fit to the data was then obtained as a

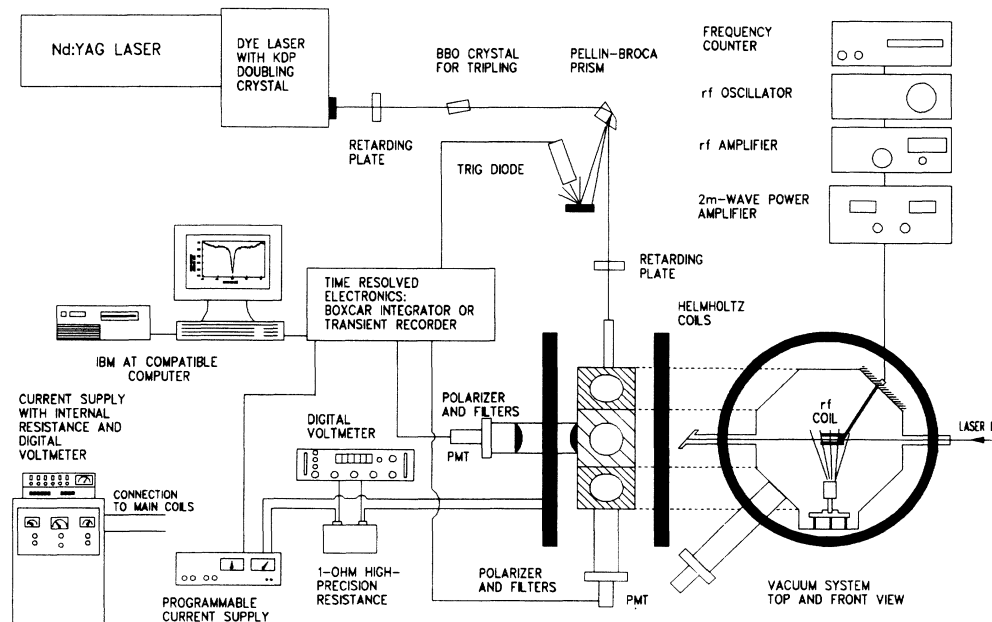


FIG. 3. Experimental setup for pulsed LC and ODR measurements. BBO, KDP, and PMT denote β -barium borate, potassium dihydrogen phosphate and photomultiplier tube, respectively.

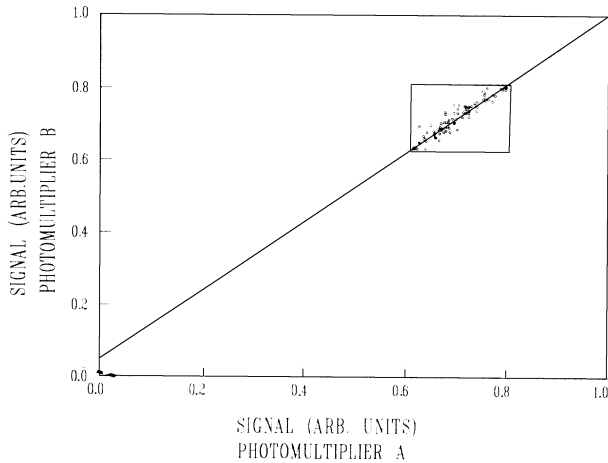


FIG. 4. Recording of dual detector data to which a linear fit has been performed as a “learning” curve.

learning curve, incorporating all the detection system imperfections. Later, in the real data recording this curve was used to rectify the data to the case of a perfect detection system.

III. MEASUREMENTS AND RESULTS

A. Level-crossing experiments

An experimental recording of the resonance $[\sigma, \sigma]$ scattering (206 nm) for the $4d^{10}6p^2P_{3/2}$ state is shown in Fig. 5. The detection polarization is set to record a symmetric line shape. A strong Hanle effect is evident centered around zero magnetic field. In the region 0.4–0.9 mT a signal depression due to four unresolved level-crossing signals (two for each isotope) occurs. The signal is best analyzed by using the known ratio between the magnetic dipole interaction constants (a) for the two isotopes and fitting only one hyperfine parameter and a lifetime to the curve. Using a computer program to calcu-

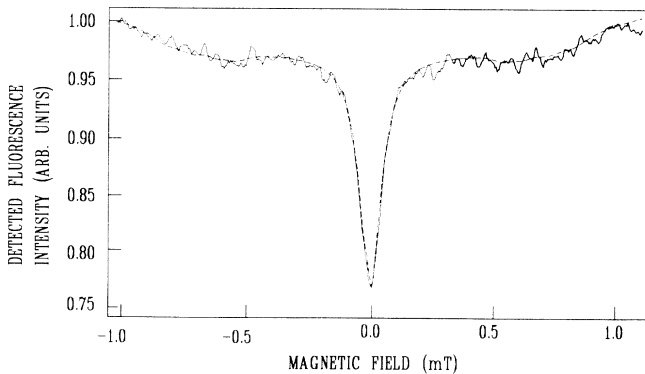


FIG. 5. Resonance scattering intensity on the $4d^{10}5s^2S_{1/2} \leftrightarrow 4d^{10}6s^2P_{3/2}$ transition at 206 nm as a function of the magnetic field. Apart from the strong Hanle signal at zero magnetic field, weak overlapping high-field crossing signals can be observed.

late the scattered intensity according to the Breit formula,^{5,17} the collected data yield $|a|=8.8(5)$ MHz for the ^{107}Ag isotope. Here a g_J factor of 1.336, as determined in the ODR experiments, was used. For the determination of the lifetime, measurements were performed at decreasing atomic densities to avoid the influence of coherence narrowing on the Hanle signal. An extrapolation to zero atomic density yields $\tau(6p^2P_{3/2})=80(4)$ ns from theoretical fits to the Hanle signal.

B. Time-resolved experiments

Using the fast microchannel plate photomultiplier tube (PMT) the decay of both the $6p^2P_{3/2}$ and $6p^2P_{1/2}$ states was recorded by scanning the gate of the boxcar integrator. A magnetic field of about 1.0 mT was applied to the atoms to wash out the slow modulation due to $\Delta F=1$ quantum beats. In Fig. 6(a) a recording is shown for the $6p^2P_{3/2}$ state. From low atomic density data we obtained $\tau(6p^2P_{3/2})=76(5)$ ns. The error comprises two standard deviations of the data. As a best value for the lifetime for this state we obtained the mean from the Hanle-effect and the time-resolved measurements $\tau(6p^2P_{3/2})=78(5)$ ns.

If instead the earth’s magnetic field is canceled using auxiliary coil systems, zero-field quantum beats are recorded.^{21,22} The Fourier transform obtained has a major peak, corresponding to the unresolved $\Delta F=1$ beats differing in frequency by 15% for the two isotopes. For ^{107}Ag the result $a=|8.8(10)|$ MHz is obtained. Corresponding time-resolved measurements for the $6p^2P_{1/2}$ state were performed using two geometries. For the lifetime measurements linear polarized light was used for excitation and in the detection step. Then for a $J=\frac{1}{2}$ state no quantum beats can be observed. Thus the exponential decay is not perturbed. From decay curves such as the one shown in Fig. 6(b) we obtained the lifetime value $\tau(6p^2P_{1/2})=95(6)$ ns, where the error comprises two standard deviations of the data.

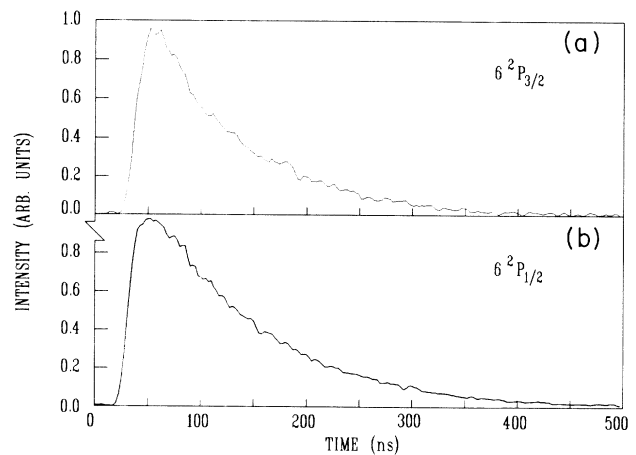


FIG. 6. (a) Time-resolved fluorescence decay curve for the $6p^2P_{3/2}$ state. (b) Time-resolved fluorescence decay curve for the $6p^2P_{1/2}$ state.

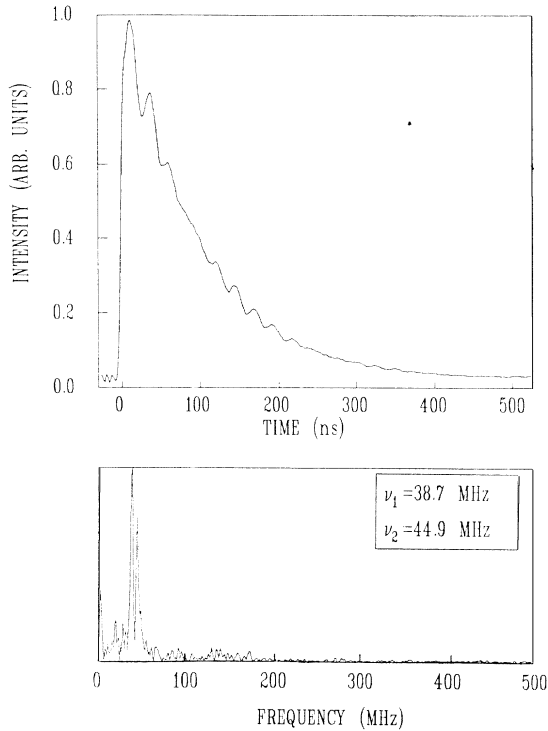


FIG. 7. Time-resolved fluorescence decay curve for the $6p\ ^2P_{1/2}$ state in silver, with superimposed quantum beats. The corresponding Fourier transform is also included.

In order to determine the hfs for the $6p\ ^2P_{1/2}$ state, circularly polarized light was used for excitation and in the detection step. If the propagation vectors have parallel components, quantum beats occur. For these experiments a transient recorder, sampling at 1 GHz, was used to record the fluorescence. To evaluate the hyperfine structure the curves were Fourier transformed (Fig. 7). The two observed frequency components originate from the two isotopes. The lower frequency, which is equal to the magnetic-dipole interaction constant for the ^{107}Ag isotope, was determined to $|a(6p\ ^2P_{1/2}\ ^{107}\text{Ag})| = 38.7(10)$.

C. Optical-double-resonance experiments

Above we have described two types of experiment that yield the hfs of the $6p\ ^2P_{3/2}$ state of silver. However, the most precise determination was made in ODR measurements in the Paschen-Back region of the hyperfine structure. Using π excitation ($\Delta m = 0$) the $m_j = \pm 1/2$ levels were populated. In the decay, π as well as σ light ($\Delta m = \pm 1$) is emitted. If $\Delta m_j = \pm 1$, magnetic-dipole transitions are driven by the rf field the $m_j = \pm 3/2$ states are populated. Since atoms in these states can only decay in σ transitions, the presence of rf resonance is manifested in a strong increase in the σ light, which is detected in the direction of the magnetic field.

For practical reasons, the magnetic field was swept through resonance rather than sweeping the radio frequency. In Fig. 8 ODR signals are shown for a resonance frequency of 145.13 MHz. Since considerably more stray

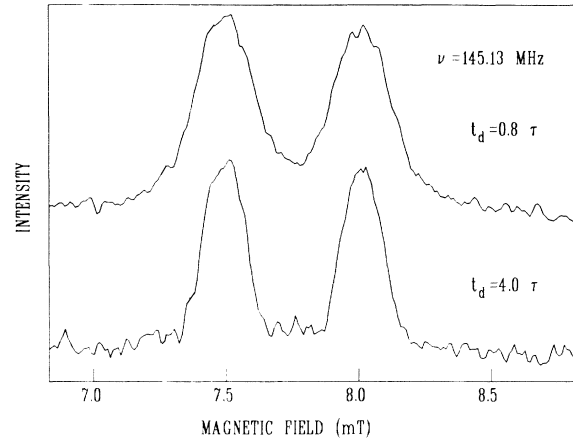


FIG. 8. ODR signals for the $6p\ ^2P_{3/2}$ state at two different detection time delays. Two rf signals are observed for near Paschen-Back region conditions.

light was observed in the ODR than in the LC experiments, because of the closeness of the rf coil to the resonance volume, the detection was delayed by 0.8τ , while all the decay was observed in the LC experiments. By delaying the detection even more, a substantial narrowing of the signals was obtained, as shown in Fig. 8 for a delay of 4τ . By restricting the detection to “old” atoms an increase in spectroscopic resolution can be obtained. This has been studied by several authors.^{23–28} Normally, the quality of the delayed data is severely impaired by oscillations in the wings of the narrowed-down signals. However, with the rise time of the PMT used, self-apodization is obtained, eliminating the oscillations. The signal-to-noise ratio for substantial delays was not determined by photon statistics, but rather by residual pulse to pulse fluctuation. Thus a reduction of the width could be obtained by detecting old atoms without much decrease in the signal-to-noise ratio. From the separation of the two signals the magnetic-dipole interaction constant was determined using data recorded at different delays:

$$|a(6p\ ^2P_{3/2}\ ^{107}\text{Ag})| = 9.05(25)\ \text{MHz}.$$

The Landé g_j factor was determined from the center of gravity of the two signals: $g_j(6p\ ^2P_{3/2}) = 1.336(2)$. The error is primarily determined by statistical scattering. The magnetic field was determined by optical pumping signals in ^{133}Cs to an accuracy of two parts in 10^4 . In the hfs as well as in the g_j determination a small deviation from pure Paschen-Back conditions was taken into account.

IV. DISCUSSION

In the present paper, as in a previous one,⁵ the usefulness of pulsed level-crossing spectroscopy for hfs studies of states reachable only by short-wavelength radiation is demonstrated. In addition, the ODR technique was employed yielding even better data. QB spectroscopy was applied to a $J = \frac{1}{2}$ state, for which special geometrical and polarization conditions pertain. New information for the

TABLE I. Magnetic-dipole interaction constants (a factors) for the $5p^2P$ and $6p^2P$ states of ^{107}Ag and the $4p^2P$ and $5p^2P$ states of ^{63}Cu . Experimental values are compared with theoretical calculations using the HF and MCHF methods.

State	a factor (MHz)		
	HF	MCHF	Experiment
$^{107}\text{Ag}(5p^2P_{3/2})$	-15.2	-25.1	-31.7(5) ^b
$^{107}\text{Ag}(5p^2P_{1/2})$	-76.1	-119	-175.4(17) ^b
$^{107}\text{Ag}(6p^2P_{3/2})$	-4.3	-9.8	$\mp 9.05(25)$ ^c
$^{107}\text{Ag}(6p^2P_{1/2})$	-21.3	-18.4	$\mp 38.7(10)$ ^c
$^{63}\text{Cu}(4p^2P_{3/2})$	55.5	225	194.72(15) ^d
$^{63}\text{Cu}(4p^2P_{1/2})$	278	368	506.6(10) ^e
$^{63}\text{Cu}(5p^2P_{3/2})$	15.9	60	61.7(9) ^f
$^{63}\text{Cu}(5p^2P_{1/2})$	79.5	259	334.6(37) ^e

^aReference 7.

^dReference 31.

^bReference 11.

^eReference 4.

^cThis work.

^fReference 5.

little-studied silver atom has been obtained.

The new data and some related results for silver and copper will now be compared with the results from theoretical calculations. The radiative lifetime and the hyperfine structure of the silver states were calculated⁷ using radial wave functions obtained with the multiconfiguration Hartree-Fock method.²⁹ To obtain reliable mixing coefficients, the configuration-average energies for higher-lying configurations have been manually corrected for before diagonalization. Nonrelativistic radial functions were used, but relativistic effects are included to the first order in the energy matrix, before diagonalization. This is the same scheme that has been used for copper in a previous paper by Carlsson.⁶ From the wave functions generated for copper, theoretical hyperfine-structure parameters have previously been calculated.⁵ However, due to a hardware error on the printer, some of the mixing coefficients have the wrong sign.³⁰ These coefficients were manually fed into the program with which the hyperfine structure parameters for the $4p^2P$ and $5p^2P$ states were calculated, and hence the agreement with experimental results was poor. Using the correct coefficient signs, the agreement for copper is improved. The calculated hyperfine-structure values for the $5p$ and $6p^2P$ levels in silver as well as the $4p$ and $5p^2P$ levels in copper are compared with Hartree-Fock and ex-

TABLE II. Radiative lifetimes for the $5p^2P$ and $6p^2P$ states of neutral silver. Experimental results are compared with a MCHF calculation.

State	Radiative lifetime (ns)	
	Theory ^a	Experiment
$\text{Ag}(5p^2P_{3/2})$	5.8	6.79(3) ^b
$\text{Ag}(5p^2P_{1/2})$	6.3	7.41(4) ^b
$\text{Ag}(6p^2P_{3/2})$	34	78(5) ^c
$\text{Ag}(6p^2P_{1/2})$	39	95(6) ^c

^aReference 7.

^bReference 11.

^cThis work.

perimental values in Table I. It can be observed that the agreement between the MCHF and experimental values for the $^2P_{3/2}$ states in both atoms is good. The $^2P_{1/2}$ states are much more sensitive to neglected relativistic effects and the experimental and theoretical values show a larger discrepancy. This is most obvious for the heavier Ag atom. However, it should be noted that in the theoretical calculation of the hfs parameters, the only contributions included were those from matrix elements involving states with the same LS designation; thus cross terms were neglected. This may be important, especially for the more perturbed Cu atom. The experimental and theoretical lifetimes for the $5p$ and $6p^2P$ states of silver are compared in Table II. It can be seen that there is a substantial difference between the calculated lifetimes and the experimental ones, calling for further developments in the theory. In order to better understand the origins of the deviations, studies on the higher 2P states of silver and copper would be desirable. In order to reach such states, vuv excitation wavelengths are needed. Experiments of that kind using short-wavelength radiation generated with nonlinear optical techniques³² should be possible.

ACKNOWLEDGMENTS

The authors would like to thank J. Carlsson, P. Jönsson, and C. -G. Wahlström for valuable discussions concerning the theoretical interpretation. This work was supported by the Swedish Natural Science Research Council.

¹C. Moore, *Atomic Energy Levels*, Natl. Stand. Ref. Data Ser. No. 35, Natl. Bur. Stand. (U.S.) (U.S. GPO, Washington, D.C., 1971).

²H. -U. Johannsen and R. Lincke, *Z. Phys. A* **272**, 147 (1974).

³J. Carlsson, A. Dönszelmann, H. Lundberg, A. Persson, L. Sturesson, and S. Svanberg, *Z. Phys. D* **6**, 125 (1987).

⁴H. Bergström, W. X. Peng, and A. Persson, *Z. Phys. D* **13**, 203 (1989).

⁵J. Bengtsson, J. Larsson, S. Svanberg, and C. -G. Wahlström, *Phys. Rev. A* **41**, 233 (1990).

⁶J. Carlsson, *Phys. Rev. A* **38**, 1702 (1988).

⁷J. Carlsson and P. Jönsson (private communication).

⁸L. A. Levin and B. Budick, *Bull. Am. Phys. Soc.* **11**, 455 (1966).

⁹H. Bucka, D. Einfeld, J. Ney, and J. Wilken, *Z. Naturforsch.* **26A**, 1016 (1971).

¹⁰M. Soltanolkotabi and R. Gupta, *Phys. Lett.* **96A**, 399 (1983).

¹¹J. Carlsson, P. Jönsson, and L. Sturesson, *Z. Phys. D* **16**, 87 (1990).

¹²G. L. Plekhotkina, *Opt. Spectrosc.* **51**, 106 (1981).

¹³Jiang Zhankui, P. Jönsson, J. Larsson, and S. Svanberg (to be published).

¹⁴H. E. Walchilli, Oak Ridge National Laboratory Report No.

- ORNL-1469, Suppl. II, 1955 (unpublished).
- ¹⁵F. D. Colgrove, P. A. Franken, R. R. Lewis, and R. H. Sands, *Phys. Rev. Lett.* **3**, 420 (1957).
- ¹⁶P. A. Franken, *Phys. Rev.* **121**, 508 (1961).
- ¹⁷G. Breit, *Rev. Mod. Phys.* **5**, 91 (1933).
- ¹⁸W. Happer and R. Gupta, in *Progress in Atomic Spectroscopy*, edited by W. Hanle and H. Kleinpoppen (Plenum, New York, 1978).
- ¹⁹J. Brossel and F. Bitter, *Phys. Rev.* **86**, 368 (1952).
- ²⁰U. Wolf and E. Tiemann, *Appl. Phys. B* **39**, 35 (1986).
- ²¹J. N. Dodd and G. W. Series, in *Progress in Atomic Spectroscopy*, edited by W. Hanle and H. Kleinpoppen (Plenum, New York, 1978), Part A, p. 639.
- ²²S. Haroche, in *High-Resolution Laser Spectroscopy*, Vol. 13 of *Topics in Applied Physics*, edited by K. Shimoda (Springer, Heidelberg, 1976), p. 253.
- ²³P. Schenck, R. C. Hillborn, and H. Metcalf, *Phys. Rev. Lett.* **31**, 189 (1973).
- ²⁴H. Figger and H. Walther, *Z. Phys.* **267**, 1 (1974).
- ²⁵J. S. Deech, P. Hannaford, and G. W. Series, *J. Phys. B* **7**, 1311 (1975).
- ²⁶P. D. O'Brien, P. Meystre, and H. Walther, in *Advances in Atomic and Molecular Physics*, edited by D. Bates and B. Bedersson (Academic, Orlando, 1985), Vol. 21.
- ²⁷J. Larsson, L. Sturesson, and S. Svanberg, *Phys. Scr.* **40**, 165 (1989).
- ²⁸F. Shimizu, K. Shimui, Y. Gomi, and H. Takuma, *Phys. Rev. A* **35**, 3149 (1987).
- ²⁹C. Froese Fischer, *The Hartree-Fock Method for Atoms* (Wiley, New York, 1977).
- ³⁰J. Carlsson (private communication).
- ³¹J. Ney, *Z. Phys.* **196**, 53 (1966).
- ³²S. Svanberg, in *Applied Laser Spectroscopy*, edited by M. Inguscio and W. Demtröder (Plenum, New York, in press).